Axial Dispersion in Packed Beds with Large Wall Effect

BUM-JONG AHN and ANDRÉ ZOULALIAN

Université de Technologie de Compiègne
Compiègne, France

J. M. SMITH
University of California
Davis, CA 95616

INTRODUCTION

Axial dispersion in packed beds has been extensively studied for large ratios of tube to particle diameter (Froment and Bischoff, 1979, and Wakao and Kaguei, 1982, provide recent reviews). Less information is available for beds in which the particle size is of the same order of magnitude as the tube diameter. For relatively large particles in small tubes with ratios (d_t/d_p) of 1.1 to 1.4, Scott et al. (1974) found that axial dispersion Peclet numbers are not much less than when the ratio is large (>15). However, when the ratio is somewhat greater than 1.4, axial dispersion appears to be much greater. Hsiang and Haynes (1977) found axial Peclet numbers for beds of large particles (ratio < 8) to be much less than expected from correlations neglecting the wall effect. Thus Pe_∞ for high fluid flow rates was considerably less than 2. In this paper additional data are presented for d_t/d_p from 1.9 to 4.7. In addition to the experimental data, which agree in general with the Hsiang and Haynes results, an approximate expression is proposed for the explicit effect of d_t/d_p on the Peclet number at high flow rates. Prior correlations (e.g., Edwards and Richardson, 1970; Urban and Gomezplata, 1969) do not include an explicit function of d_t/d_p. Axial dispersion at intermediate values of d_t/d_p and high flow rates is of practical interest in some packed-bed processes, for example, when large radial heat transfer rates are required. Pressure drop increases as the flow rate increases and this causes density changes in the bed. However, this effect is diminished due to the large void fractions in the beds used in our work.

EXPERIMENTAL

Axial dispersion was determined by pulse-response measurements over a range of flow rates (Reynolds number from 1 to 200) in columns of three different diameters (0.0085 to 0.0212 m) at 293 and 473 K and atmospheric pressure. The packed test section was 0.3 m long, with an additional 0.15 m packed calming section prior to the test section and another 0.15 m section after the test region. Figure 1 is a schematic drawing of the apparatus. The tubes were packed with irregular shaped, granular particles with an average size of 0.0045 m and porosity of 0.537. The particles were porous and consisted of copper stabilized oxides of vanadium (VO_6) and phosphorous (PO_4). The chemical structure of the particles is described by Ahn (1980) and Rodriguez et al. (1982). The d_t/d_p ratios and void fractions ϵ of the three columns are given in Table 1. The ϵ values are very high compared with void fractions in beds packed with smooth particles. Thus the pressure drop over the test section was low, about 10^{-2} m of water. With these conditions, the density change was negligible up to velocities of the order of 1.0 m/s.

Pulses of hydrogen in air (as the carrier gas) were introduced upstream of the columns and detected at both entrance and exit of the test section using a mass spectrometer, Micromass Co., Model 601. Details of the apparatus are described by Ahn (1980). For the same gas flow rate, response curves (C vs. t) were measured at two locations along the center line of the column for each run, first with the detector at the entrance to the test section and then with the detector at the end of the test section. Hence, the input curves measured at the entrance of the test section were already dispersed due to the entrance and calming sections. The measured output responses at the exit of the test section were further flattened due to axial dispersion and intraparticle diffusion. Typical response curves are shown in Figure 2.

Both input and output curves include responses, in series, of the sampling lines and detector. As shown in Figure 1, the sample lines were identical in both the entrance and exit of the test section. Also, the response time of the mass spectrometer detector was of the order of 10^{-3} s. Hence, the responses of the sampling lines and the instrument were the same and essentially linear. Under these conditions the transfer function $\bar{C}_L/\bar{C}_o$ determined from the entrance and exit response curves was free of distortion due to the responses of the instrument and sample lines.

The pulse was injected via a six-way chromatographic-type valve operated pneumatically and activated by a solenoid value. The latter was connected to a common switch with the zero time marker on the spectrogram. This arrangement synchronized zero time on the input and output curves.

The response curves were digitalized semimanually with a graphic terminal, HP Model 2647A. These response curves at the inlet and outlet of the test section were transformed to the Laplace domain by numerical integration, leading to values of $\bar{C}_L/\bar{C}_o$ as functions of the Laplace variable, s.

ANALYSIS AND RESULTS

Consider the flow of carrier gas, containing a nonadsorbing tracer, through a packed bed of porous particles. Suppose that the flow is represented by an axial dispersion model with intraparticle diffusion. The mass balance of tracer in the interparticle space may be written

$$D_a \frac{\partial^2 C}{\partial z^2} = u \frac{\partial C}{\partial t} + (1-\epsilon)\beta \frac{\partial \langle C' \rangle}{\partial t} \tag{1}$$

where u is the superficial velocity (constant) in the axial z)

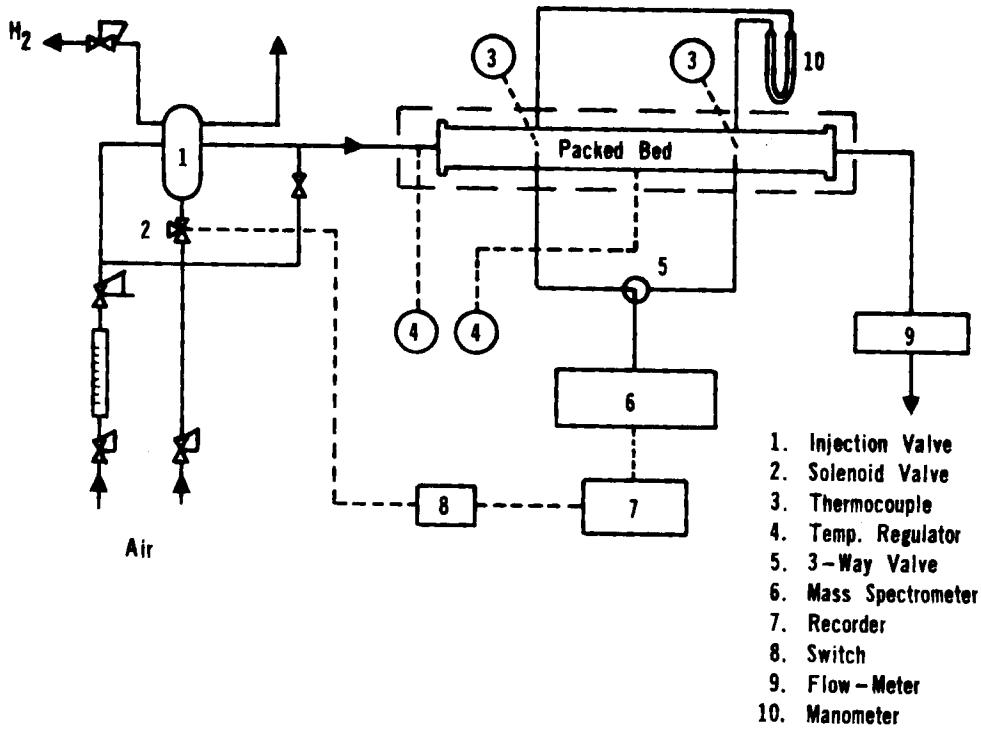

Figure 1. Schematic drawing of apparatus.

direction, and the last term is the accumulation of tracer in the pore volume of the particles. The boundary conditions are

$$\text{for } z = 0,\ C(t) = C_0(t) \tag{2}$$

$$\text{for } z = \infty,\ C(t) \text{ is finite} \tag{3}$$

The mass balance of tracer in the particles, for a slab of thickness $2x_o$, is

$$D_e \frac{\partial^2 C'}{\partial x^2} = \beta \frac{\partial C'}{\partial t} \tag{4}$$

with boundary conditions:

$$\text{at } x = x_0 \text{ (center of slab)},\ \frac{\partial C'}{\partial x} = 0 \tag{5}$$

$$\text{at } x = 0 \text{ (face of slab)},\ C'(t) = C(t) \tag{6}$$

The initial condition is $C = 0$ and $C' = 0$ for all z and x. Since the gas flow rate was large enough that mass transfer resistance between bulk gas and particle surface was negligible (Ahn, 1980), Eq. 6 was applicable.

Equations 1 to 6 can be made dimensionless with respect to z and x and solved in the Laplace domain to obtain the following transfer function $G(s)$ for the test section:

$$G(s) = \left[\exp\frac{Pe(\lambda)}{2} \times \left\{1 - \sqrt{1 + \frac{4\tau s}{Pe(\lambda)}\left(\epsilon + (1-\epsilon)\beta\frac{\tanh(s\tau_d)^{1/2}}{(s\tau_d)^{1/2}}\right)}\right\}\right] \tag{7}$$

In this expression τ is the residence time, L/u, in the bed; τ_d is the intraparticle diffusion time, $\beta x_o^2/D_e$; and λ is the length-to-particle size ratio L/d_p.

By equating $G(s)$ from Eq. 7 to $\bar{C}_L/\bar{C}_o$ determined from the experimental response curves, the two parameters Pe and τ_d can

Table 1. Peclet Numbers At High Flow Rates

d_t, m	d_t/d_p	ϵ	Pe_∞
0.0212	4.7	0.676	0.14
0.0157	3.5	0.692	0.18
0.0085	1.9	0.709	1.00

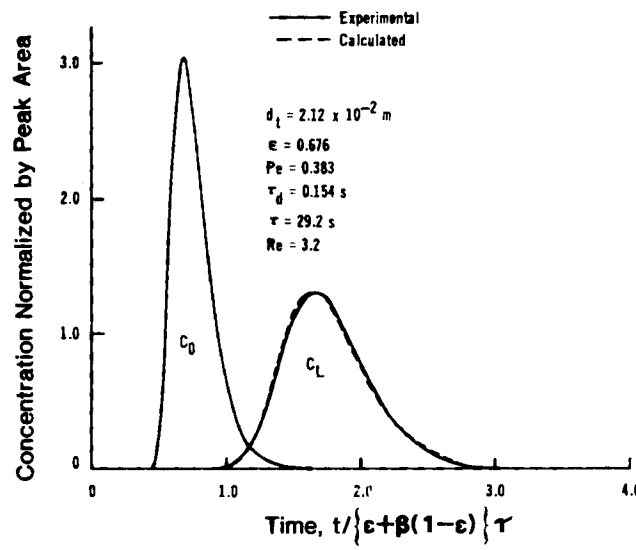

Figure 2. Experimental and calculated response curves.

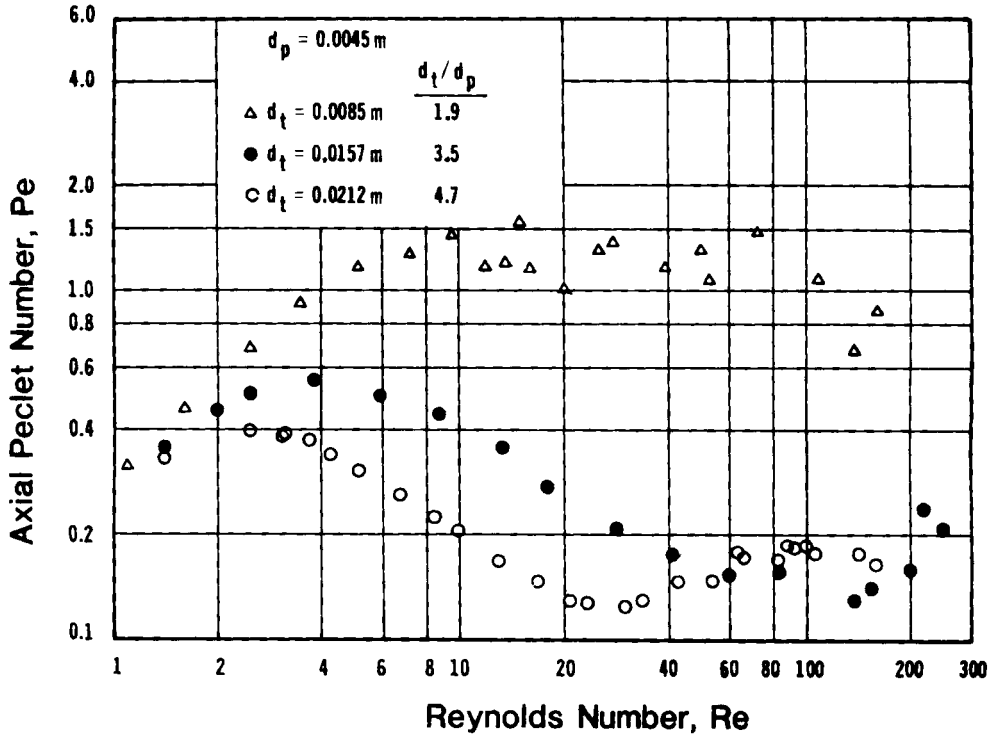

Figure 3. Axial Peclet numbers at 293 K.

be determined. This was done using a two-parameter optimization technique for dimensionless values of $s\tau$ from 0.2 to 4. Wakao and Kaguei (1982) have found that $s\tau$ values in this range are best for evaluating rate parameters from dynamic data. The diffusion times were found to be 0.287 s t 293 K and 0.136 s at 473 K. These values, using an eqivalent slab half-thickness of $d_p/6$, correspond to effective diffusivities of 1.1×10^{-6} m^2/s at 293 K and 2.2×10^{-6} m^2/s at 473 K. The Peclet numbers, plotted in Figures 3 and 4, showed the same dependency on Reynolds number at both temperatures and were about the same in magnitude. The latter agreement confirms the assumption of negligible adsorption of hydrogen made in writing Eqs. 1 and 4.

For all d_t/d_p ratios, the Peclet numbers in Figures 3 and 4 go through a maximum and then become nearly constant as the Reynolds number increases. The data points for the smallest tube (d_t/d_p = 1.9) give Pe values similar to those reported by Hsiang

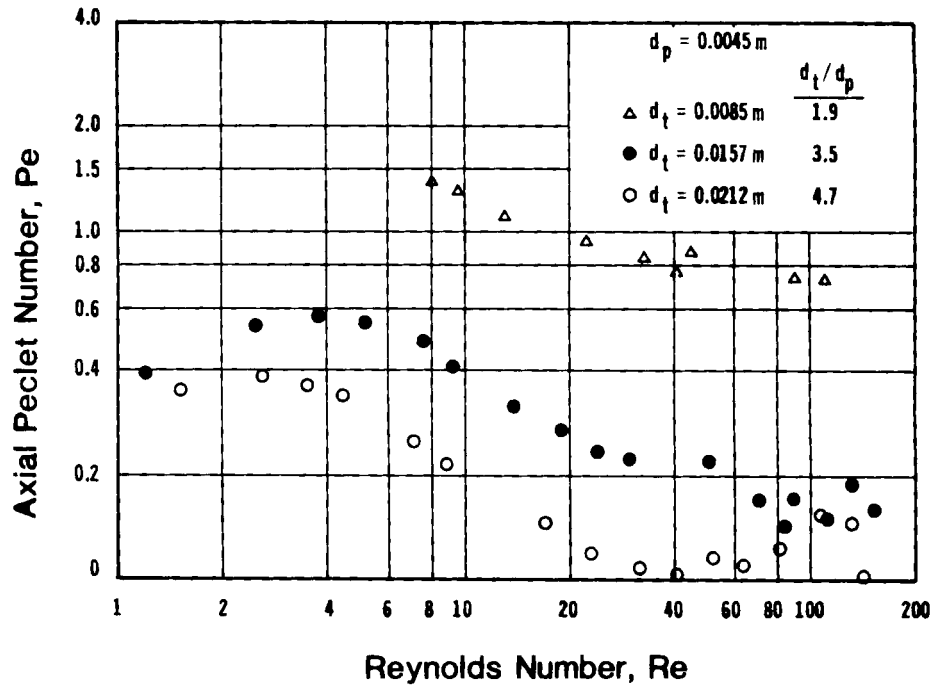

Figure 4. Axial peclet numbers at 473 K.

and Haynes (1977) for low ratios. However, for the larger tubes (ratios of 3.5 and 4.7) the data show much lower Peclet numbers corresponding to much stronger axial dispersion. This is also shown in Table 1 where average values (considering both temperatures) of Pe at $Re > 20$ are listed for each tube.

Effect of d_t/d_p on Peclet Number at Large Re

Radial variation in void fraction due to the tube wall and the corresponding velocity variation has been well established (Stanek and Eckert, 1979; Schwartz and Smith, 1953). The channeling of the flow can enhance axial dispersion in the model used to formulate Eq. 1.

It is proposed to account approximately for the wall effect (at large flow rates and for nonporous particles) by applying the two-region flow model employed by Oliveros and Smith (1982). In this model it is supposed that the bed consists of a cylindrical core and a surrounding annulus with different void fractions, ϵ. No mixing is permitted between the two regions. Suppose that the fraction of volumetric flow in the annulus is W, and 1-W is the flow in the core. Then the first and second moments, μ_1 and μ_2, of the response curve for the combined effluent can be written

$$\mu_1 = (1 - W)\mu_1^c + W\mu_1^a \tag{8}$$

$$\mu_2 = (1 - W)\mu_2^c + W\mu_2^a \tag{9}$$

For a packed bed the variance δ^2 can be related to the Peclet number using Eq. 7. The limit of the first derivative of $G(s)$ as $s \to 0$ gives the first moment. Using Eq. 7 for nonporous particles ($\tau_d = 0$), the result is

$$\mu_1 = \epsilon t \tag{10}$$

Similarly, the limit of the second derivative gives μ_2:

$$\mu_2 = (\epsilon\tau)^2 + \frac{2(\epsilon\tau)^2}{(Pe)(\lambda)} \tag{11}$$

With Eq. 10, Eq. 11 becomes

$$\delta^2 = \mu_2 - \mu_1 = \frac{2\mu_1^2}{\lambda(Pe)} \tag{12}$$

If both the annulus and core are approximated with no wall effect, $Pe_\infty = 2$ for high flow rates. Then Eq. 12, applied to each region gives

$$\mu_2^c = \left(1 + \frac{1}{\lambda}\right)(\mu_1^c)^2 \text{ and } \mu_2^a = \left(1 + \frac{1}{\lambda}\right)(\mu_1^a)^2 \tag{13}$$

Substituting Eq. 13 into Eq. 9 eliminates the second moments. Then using Eqs. 8 and 9 in Eq. 12 gives an equation involving first moments μ_1^c and μ_1^a.

Solving this expression for Pe_∞ yields

$$Pe_\infty = \frac{2/\lambda}{\dfrac{(1 + \lambda)(1 - W + W\alpha^2)}{\lambda(1 - W + W\alpha)^2} - 1} \tag{14}$$

where

$$\alpha = \mu_1^a/\mu_1^c \tag{15}$$

Stanek and Kolar (1973) correlated the wall flow of liquid in a trickle bed in the functional form

$$W = \frac{1}{1 + \gamma f(d_t/d_p)} \tag{16}$$

For the trickle bed they chose $f(d_t/d_p) = d_t/d_p$. Assuming that this expression applies for gases, the wall flow can be approximated as

$$W = \frac{1}{1 + \gamma(d_t/d_b - 1)} \tag{17}$$

where γ is a constant, independent of d_t/d_p, to be determined from experimental data. We have taken $f(d_t/d_p) = d_t/d_p - 1$, since for gases all the flow is assumed to be at the wall when d_t/d_p is unity. With Eq. 17 for W, Eq. 14 for the Peclet number at high flow rates becomes the following function d_t/d_p, and involves α and γ,

$$Pe_\infty = \frac{2}{1 + \dfrac{1}{A\left(\dfrac{d_t}{d_p} - 1\right) + B + \dfrac{C}{(d_t/d_p) - 1}}} \tag{18}$$

where

$$A = \frac{\gamma}{(1 + \lambda)(1 - \alpha)^2} \tag{19}$$

$$B = \left(\frac{2}{1 + \lambda}\right)\frac{\alpha}{(1 - \alpha)^2} \tag{20}$$

$$C = \frac{[\alpha/(1 - \alpha)]^2}{(1 + \lambda)\gamma} \tag{21}$$

Equation 18 is proposed as an approximate relationship for correlating the effect of d_t/d_p on the Peclet number at high flow rates in a packed bed with nonporous particles. The constant γ would be found from experiment. Stanek and Kolar (1973) employed $\gamma = 0.18$ in their trickle bed study. The first moment (retention time) ratio α could be determined experimentally as described by Oliveros and Smith (1982) or determined as an arbitrary constant from data such as those presented in Figures 3 and 4.

The form of Eq. 18 is such that Pe first decreases to a minimum and then increases toward a constant value as d_t/d_p increases. This variation is in agreement with the experimental data presented here and by Hsiang and Haynes (1977). Equations 19–21 would not be applicable for large values of λ since no mixing between core and annulus was allowed for in the model.

In the model developed by Hsiang and Haynes the cross section of the bed also was divided into two regions. In our model, for which the objective is the effect of d_t/d_p on Pe, no allowance is made for mass transfer between the central core and wall region, but we did include finite velocities in each region. The Hsiang and Haynes model allowed for mass transfer between regions, but assumed that the velocity in the central core was negligible. The main purpose was to correlate the effect of superficial velocity on the Peclet number. Thus, the two models were similar but involved different assumptions and were proposed for different objectives.

ACKNOWLEDGMENT

The first author is grateful to the French Government for financial support. Also, Rhone-Poulenc Industries kindly provided porous particles.

NOTATION

$C(t)$ = fluid phase concentration, kmol/m^3
$C_o(t)$ = inlet fluid phase concentration
$C_L(t)$ = outlet fluid phase concentration

C' = intraparticle fluid concentration, kmol/m^3
$\langle C' \rangle$ = average concentration in the particle
$\bar{C}$ = Laplace transform of fluid phase concentration
D_a = axial dispersion coefficient, m^2/s
D_e = effective diffusivity, m^2/s
d_p = particle diameter, m
d_t = tube diameter, m
L = length of test section, m
Pe = Peclet number, ud_p/D_a
Pe_∞ = Peclet number at high flow rate
Re = $d_p u\rho/\mu$
s = Laplace variable, s^{-1}
t = time, s
u = superficial velocity, m/s
u_c = superficial velocity in core region
u_a = superficial velocity in annulus region
W = fraction of total volumetric flow in annulus region
x = distance measured from face of slab, m
x_o = half thickness of slab equivalent to porous particle, m
z = axial coordinate in the fixed bed, m

Greek Letters

α = ratio of the first moments in annulus and core, $\mu_1{}^a/\mu_1{}^c$
β = porosity of the particle
γ = constant in Eq. 17
ϵ = porosity of the bed
ϵ_a = porosity in the annulus region
ϵ_c = porosity in the core region
λ = ratio of bed length to particle size, L/d_p
μ_1 = first moment of response curve for the packed bed, s
$\mu_1{}^a$, $\mu_1{}^c$ = refer to the annulus and core regions
μ_2 = central second moment of response curve s^2
$\mu_2{}^a$, $\mu_2{}^c$ = refer to the annulus and core regions
δ^2 = variance of the response curve, s^2
τ = residence time in the empty bed, L/u, s
τ_d = intraparticle diffusion time, $\beta x_o{}^2/D_e$, s

LITERATURE CITED

Ahn, B. J., "Etude des Caractéristiques Diffusionnelles de Transfert de Matière dans un Réacteur Catalytique à Lit Fixe d'Oxydation Ménagée," (Study on Diffusional Characteristics of mass Transfer in a Fixed-Bed Catalytic Reactor for Partial Oxidation), Docteur-Ingénieur Dissertation, Université de Technologie de Compiègne (1980).

Edwards, M. F., and J. F. Richardson, "The Correlation of Axial Dispersion Data," *Can. J. Chem. Eng.*, **48**, 466 (1970).

Froment, G. F., and K. B. Bischoff, *Chemical Reactor Analysis and Design*, Wiley, New York, 527, (1979).

Hsiang, T. C., and H. W. Haynes, Jr., "Axial Dispersion in Small Diameter Beds of Large, Spherical Particles," *Chem. Eng. Sci.*, **32**, 678 (1977).

Oliveros, G., and J. M. Smith, "Dynamic Studies of Dispersion and Channeling in Fixed Beds," *AIChE J.*, **28**(5), 751 (1982).

Rodriquez, A. E., B. J. Ahn, and A. Zoulalian, "Intraparticle Forced Convection Effect in Catalyst Diffusivity Measurements and Reactor Design," *AIChE J.*, **28**, 541 (1982).

Schwartz, C. E., and J. M. Smith, "Flow Distribution in Packed Beds," *Ind. Eng. Chem.*, **45**, 1,209 (1953).

Scott, D. S., W. Lee, and J. Papa, "The Measurement of Transport Coefficients in Gas-Solid Heterogeneous Reactions," *Chem. Eng. Sci.*, **29**, 2,155 (1974).

Staneck, V., and V. Eckert, "A Study of the Area Porosity Profiles in a Bed of Equal-Diameter Spheres Confined by a Plane," *Chem. Eng. Sci.*, **34**, 933 (1979).

Staneck, V., and V. Kolar, "Distribution of Liquid Over a Random Packing. VII: The Dependence of Distribution Parameters on the Column and Packing Diameter," *Colln. Czech., Chem. Commun.*, **38**, 1,012 (1973).

Urban, J. C., and A. Gomezplata, "Axial Dispersion Coefficients in Packed Beds at Low Reynolds Numbers," *Can. J. Chem. Eng.*, **47**, 353 (1969).

Wakao, N., and S. Kagluei, *Heat and Mass Transfer in Packed Beds*. Gordon and Breach, New York, 7 (1982).

Manuscript received July 19, 1984, and revision received Dec. 12, 1984.